

ACCST Research Journal

ISSN 0972-7779

Volume - XXII, No. 1, January 2024

Journal website: [www.internationaljournalsiwan.com](http://www.internationaljournalsiwan.com)

ORCID Link: <https://orcid.org/0009-0008-6661-0289>

Google Scholar: <https://scholar.google.com/citations?user=KJ4eXesAAAAJ&hl=en>

Refereed and Peer-Reviewed Quarterly Journal



---

## **Deep Learning Techniques for Lung Cancer Detection in Chest X-Rays Using Lung Segmentation**

by **Avinash Kumar**, *Research Scholar*,

*Department of Mathematics (Computer Science),*

*Magadh University, Bodh Gaya - 824234, India*

E-mail: [avinashkumar241975@gmail.com](mailto:avinashkumar241975@gmail.com)

**Shyam Sundar Prasad Singh**, *Assistant Professor*,

*Department of Mathematics,*

*S.N. Sinha College, Warisaliganj - 805130, Nawada, India*

E-mail: [sspsinghrajgir@gmail.com](mailto:sspsinghrajgir@gmail.com)

(Received: December 30, 2023; Accepted: January 19, 2024;

Published Online: January 30, 2024)

### **Abstract:**

*Using chest X-rays to find lung cancer early and correctly is very important for better patient results. Problems with traditional methods include bones and soft tissues rubbing against each other, which can make it hard to see important traits in lung cancer detection. This study looks at how to improve chest X-ray analysis by combining deep learning techniques with lung segmentation and bone shadow removal methods. By using these methods, we hope to get rid of the noise and useless data in chest X-rays so that we can focus more clearly on the lung areas. For this study, we use a Convolutional Neural Network (CNN)*

**[39]**

*framework designed for medical picture analysis along with U-Net-based methods for lung segmentation. This division process separates the lung areas from the body parts around them. Also, a bone shadow elimination method is used to get rid of even more noise from ribs and clavicle shadows. This keeps the model from being side tracked by features that aren't important. The study's dataset is made up of a lot of labelled chest X-rays of people who have been diagnosed with lung cancer and people who are healthy. Our tests show that using these preparation techniques along with deep learning makes lung cancer diagnosis much more accurate, even better than using traditional chest X-ray analysis methods. Both sensitivity and specificity have gotten a lot better, which suggests that the suggested method could help doctors make better diagnoses. This way may also help AI-driven tests become more common in clinical practice, especially in places where CT scans are hard to get to.*

**Keywords:** X-ray, CNN, U-Net, Lung Segmentation

## **1. Introduction:**

The number of people with lung cancer is very high, especially in China, where more than half of adult men are affected by it. The effects of the disease are made worse by dirty air. Lung cancer is very common in China and around the world. Early screening is the current answer, and it often leads to good results at a low cost. Everyone in the world agrees that screening, especially with computed tomography, is a good way to lower the death rate from lung cancer [1]. But it doesn't get used very often because it's expensive and hard to get in most parts of the world. At this point, chest X-ray (CXR) imaging is the most common and easy-to-get screening tool for checking on health and finding lung diseases like cancer, asthma, tuberculosis, and more. But using CXRs to find signs of these diseases is a very difficult process that needs the help of experienced doctors. Long hand analysis and discovery times for lung cancer delay the use of CXRs, and there aren't enough experts to do the work. For example, more than 600,000 cases of lung cancer are identified every year in China, but only 1.4 billion people don't have access to qualified doctors. Recently, big steps forward in computing, especially computing on general purpose Graphic Processing Units (GPUs) [2, 3], machine learning, and especially deep learning [4] for picture recognition have had a big impact. For example, the CheXNet model was just released and can automatically find pneumonia on chest X-rays at a level higher



than what actual doctors can do [5]. That's why any automatic tools and machine learning methods that help find, classify, and divide up worrisome areas (like sores, lumps, etc.) more quickly and accurately are so important for the next diagnosis. The main point of this study is to show how well lung segmentation and bone shadow exclusion work for analysing 2D CXRs using a deep learning method that can help doctors find areas that look fishy in lung cancer patients.

## 2. Related Work:

Lung cancer spots that look worrisome can now be found in a number of different ways. Radiologists can make more accurate diagnoses with Computed Tomography (CT) because it is very good at finding tumours that are hard to see. Most people think of X-rays as an old way to do medical imaging, but digital tools and machine learning have made them useful again for detection. When it comes to X-ray scans, they are especially good at finding lung tumours and can pick up more types of heart and chest diseases. Machine learning and GPU computing study for medical data handling is making fast progress, which helps the results. Few months ago, machine learning and, more specifically, deep learning methods showed some hopeful results in the area of lung disease diagnosis. Since this is the case, the present GPU-based software can handle hundreds of high-resolution medical pictures instantly. Researchers can train, test, and fine-tune their new methods using open datasets that contain CT and CXR pictures. As suggested by the Japanese Society of Radiological Technology (JSRT), letting study groups around the world use a picture database with and without lung cancer tumours is a good way to do this [6]. Other study and medical institutions backed this project. There are more than 244000 images in the Lung Image Database Consortium's (LIDC) database that were taken by different imaging methods (Computed Tomography, or CT), on more than 1000 patients. The images have an in-plane resolution of  $512 \times 512$  pixels and a range of 0.542-0.750 mm [7]. For more study on computer-assisted detection of lung diseases, especially pulmonary TB [8, 9], the U.S. National Library of Medicine has made two sets of CXRs available to the public. In Maryland, USA, the Department of Health and Human Services in Montgomery County worked with the Montgomery County (MC) dataset to be created. From the Shenzhen No. 3 People's Hospital in Shenzhen, China, we got the Shenzhen Hospital dataset (SH). In both sets, there are both normal and abnormal chests X-rays with signs

of tuberculosis, along with the radiologist's notes that go with them. The Chest X-ray14 dataset has over 100,000 frontal-view X-ray pictures of people with 14 different lung diseases. It is the biggest chest X-ray collection that is open to the public [10]. It was learnt on the Chest X-ray14 dataset [5], which is where the 121-layer convolutional neural network CheXNet received its training. Investigators try to leave out areas that aren't related to lungs or other areas of interest in order to make more accurate guesses. Cutting up normal CXRs into left and right lung fields is part of this job. Recent suggestions include active shape models, active look models, and a multi-resolution pixel classification method for different ways to divide things into groups. Two human witnesses carefully separated all the items in the JSRT database [11] so that the methods could be tried. It's still hard to separate the lung fields in CXR and MRI pictures [12], even though many new segmentation methods have been suggested for their use in medical imaging. The removal of body parts that cover the lung, like the ribs and clavicles, is another potential way to improve the forecast. This bone shadow removed (BSE) form of the JSRT dataset (BSE-JSRT) was made available to the medical imaging community by the Chest Diagnostic System Research Group in Budapest, Hungary [13]. To get rid of rib shadows in CXRs, another study used a two-step algorithm. First, the ribs were defined using a new hybrid self-template method. Next, the defined ribs were suppressed using an unsupervised regression model that takes into account changes in the bone's proximal thickness along the vertical axis [14]. For the datasets used in this work, more information is given below.

### **3. Data and Methodology:**

#### **3.1 Data:**

The segmentation methods listed below were used on the JSRT and BSE-JSRT datasets. As shown in Fig. 1a, the JSRT image collection has 247 pictures, including 154 cases with lung tumours and 93 cases without them [6]. Fig. 1b shows 247 pictures from the JSRT dataset that do not have the collarbone and rib shadows erased by the special methods [13]. The work's purpose was to see what the difference was between using deep learning on the original JSRT dataset and the BSE-JSRT dataset, which is the same JSRT dataset but doesn't have the collarbone and rib shadows. The UNet-based Convolutional Neural Network (CNN) was used to separate the left and right lung areas from the heart and other parts of normal



cardiograms. Its CNN architecture makes image segmentation fast and accurate, and it showed high accuracy on several challenges, such as tracking cells from transmitted light microscopy [15], finding cavities in bitewing radiographs, and segmenting neuronal structures in electron microscopic stacks [16]. For example, this method was recently used successfully to separate lungs on CXRs from the MC and JSRT datasets using masks that were made by hand [16]. More than that, the study wanted to see what happened when the lungs were separated in order to use the deep learning method on the original JSRT dataset after separation and the same BSE-JSRT dataset after separation.



**Fig. 1(a)**

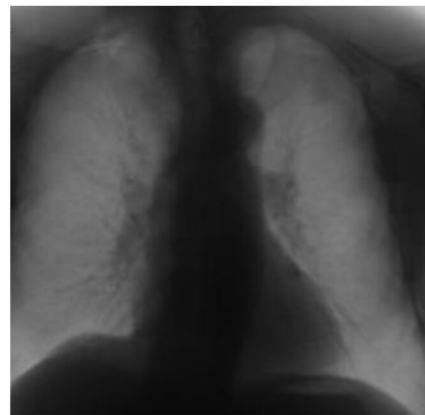


**Fig. 1(b)**

**Fig. 1:** This is an example of the original picture (2048×2048 pixels) from the JSRT dataset [6] with the cancer tumour (a), the image that goes with it from the BSE-JSRT dataset [13] without the bones (b), and the meta-information that goes with it (c). The point and circle show where the nodule is located and the area it covers (a).

### 3.2 Methodology:

We chose a simple training model with a short running time so that we could study the effects of segmentation and bone removal only in a simplified configuration. We didn't focus on getting the best accuracy and least amount of loss, which is something that will be looked into in more detail in future works. The original, divided, and bone-removed datasets, along with a simple and standard CNN model with only 7 convolution 2D layers, were used to train the model. After many tests with images of different sizes and batches in "single-CPU" (1 core of Intel i7),

“multi-CPU” (8 cores of Intel i7), and “GPU” (Graphics Processing Unit - NVIDIA Tesla K40c” modes, the running time (Fig. 2) and speedup analysis (Fig. 3) were done. For the largest picture sizes ( $1024 \times 1024$ ) and a batch size of 8 photos, the results showed a speedup of up to 9.5 times in GPU mode and 3.0 times in multi-CPU mode. The data helped us figure out what kinds of real-life situations would be good for testing the viability of segmentation and bone removal methods. Finally, the  $256 \times 256$  images were used for the previous training and are reported here. The more complex models are now being trained on the larger pictures, which will be reported elsewhere [17].

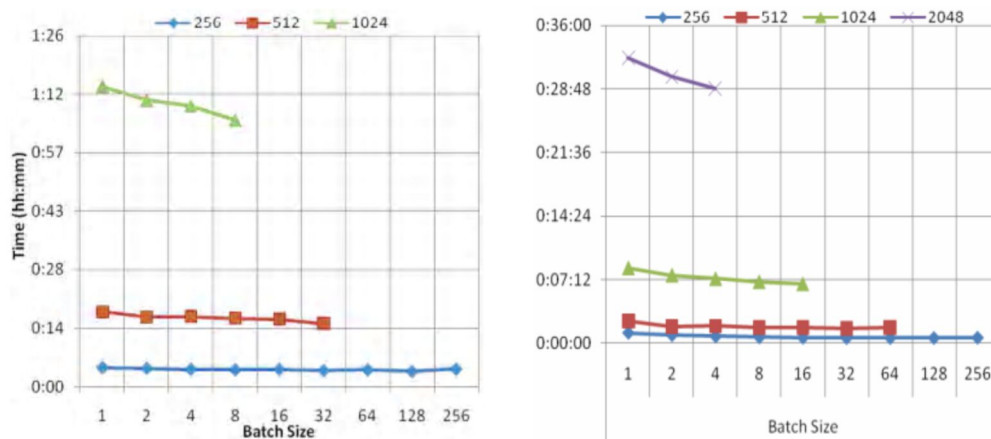


**Fig. 2: Processing time on the CPU (a) and GPU (b) for different group and picture sizes.**

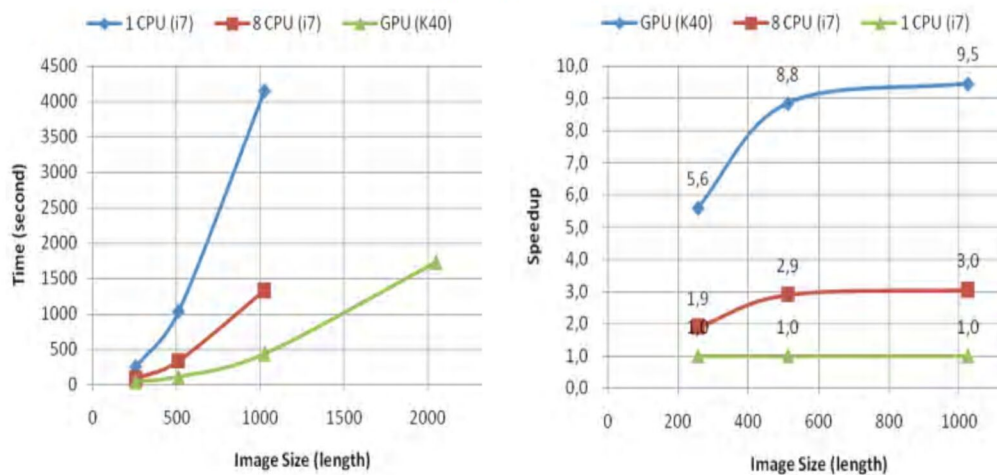


**Fig. 3: Multiple CPU and GPU modes are faster than single CPU mode**

#### 4. Results:

Here, we show the results of how bone removal and lung segmentation affected training for the original JSRT dataset, the BSE-JSRT dataset (which is the same JSRT dataset but without clavicle and rib shadows, the original JSRT dataset after segmentation, and the same BSE-JSRT dataset after segmentation.

##### 4.1 Segmentation:

This segmentation stage was applied to the original images from JSRT dataset (dataset #01, Fig. 4a) to obtain their segmented versions (dataset #03, Fig. 4c) and consisted in the following stages: training the UNet-based CNN for lung segmentation (search of lungs borders) on MC dataset with manually prepared masks (lung borders), predicting the lung borders in the shape of black-and-white lung masks (Fig. 4b) by means of the trained UNet-based CNN for each of original images from JSRT dataset (Fig. 4a), cutting the regions of interest (right and left lungs) (Fig. 4c) from their original images (Fig. 4a)

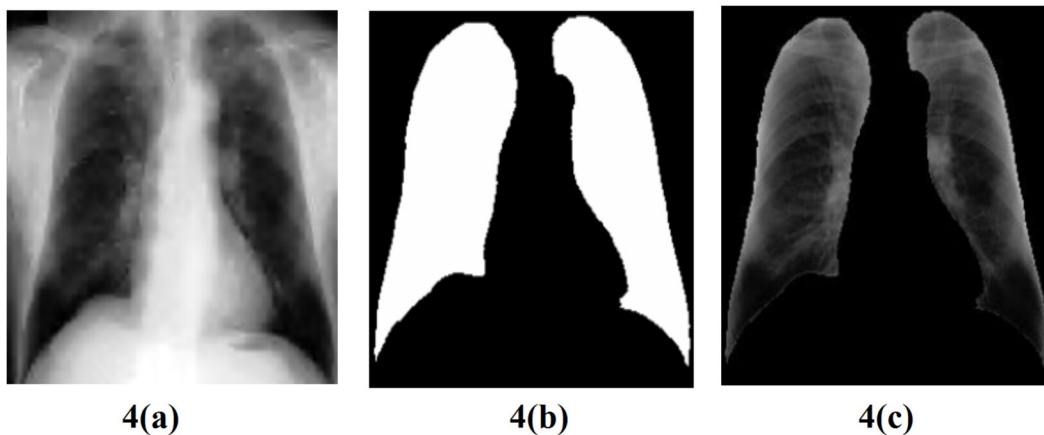


**Fig. 4:** Example of the original image (inversed version of Fig.1a) (a), the correspondent lung mask predicted by machine learning approach (b), and its segmented version (c).

##### 4.2 Training and Validation:

The basic CNN was trained in GPU mode using an NVIDIA Tesla K40c card through the Tensor Flow machine learning framework, focussing on four datasets:



the original JSRT dataset, the original BSE-JSRT dataset, which is the same as the JSRT dataset but excludes clavicle and rib, shadows the JSRT dataset post-segmentation, and the BSE-JSRT dataset post-segmentation. The prior findings (Fig. 5) clearly illustrate the significant disparity in training and validation outcomes between the unprocessed data, namely the original JSRT, and any of the pre-processed datasets. Although the original JSRT dataset 01 (red line in Fig. 5) exhibits no evidence of training due to its low image resolution and minimal nodule size, the pre-processed datasets (orange, dark blue, and blue lines in Fig. 5) display a propensity for training, achieving high training accuracy and low loss in the later stages of this simplified configuration.

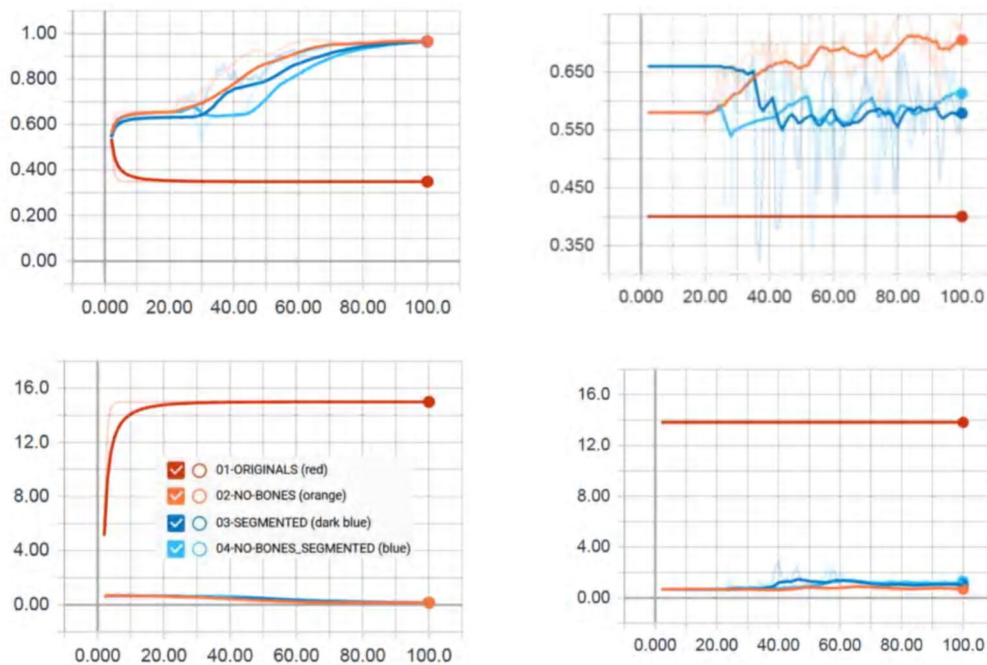


**Fig. 5:** There are four sets of data: the original images (line 01), the images without bones (line 02), the segmented images (line 03), and the segmented images without bones (line 04). The data shows the training accuracy (a), the validation accuracy (b), the training loss (c), and the validation loss (d).

## 5. Discussion and Conclusion:

The outcomes show how useful pre-processing methods like bone shadow



removal and segmentation are, especially when training in a very simple setup. The overtraining effect, which shows lower validation accuracy and higher validation loss compared to training accuracy and loss, is thought to be connected to training to artefacts like the shape of the lungs and the pattern of the edges of the lungs.

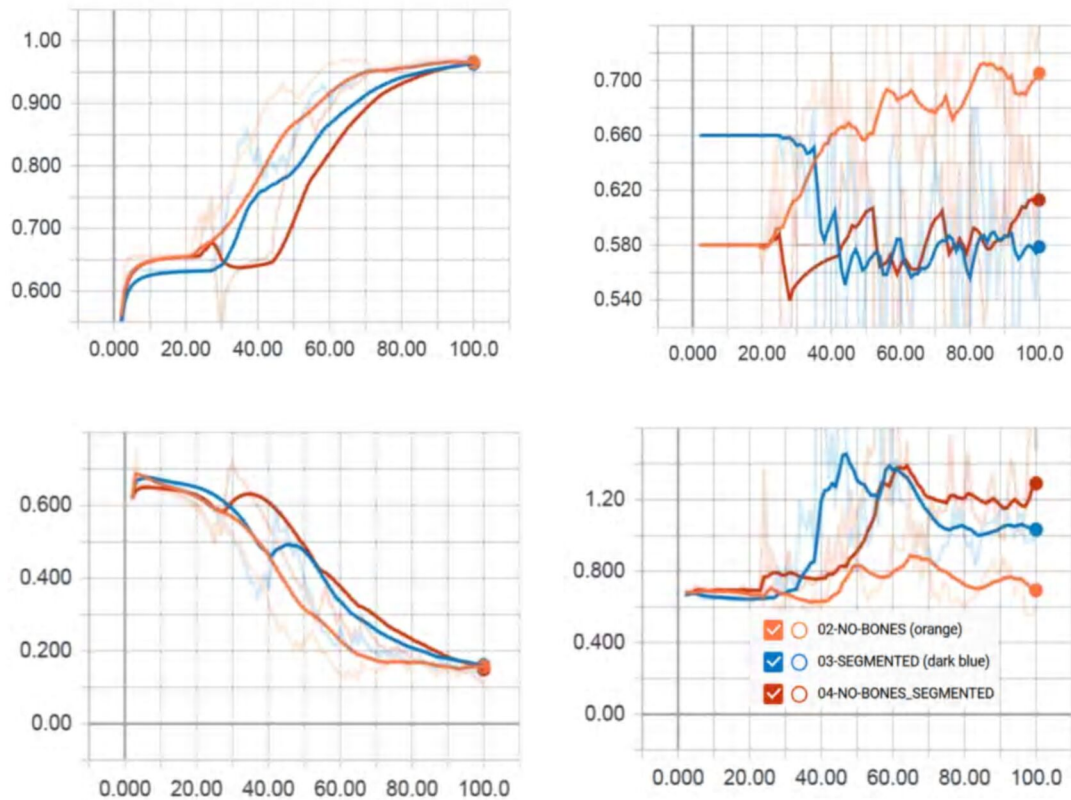


**Fig. 6:** The following are the metrics for the pictures without bones (line 02), the segmented images (line 03), and the segmented images without bones (line 04): training accuracy (a), validation accuracy (b), training loss (c), and validation loss (d).

The investigated datasets could be made bigger: the image size could go from the current  $256 \times 256$  values to  $1024 \times 1024$  (Chest X-Ray dataset) and  $2048 \times 2048$  (JSRT dataset); the number of images could go from the current 247 (JSRT and BSE-JSRT datasets) to  $>1000$  (MC dataset) and  $>100,000$  (Chest X-Ray dataset); and the data could be made bigger in terms of lossy and lossless transformations

[17]. A lot more progress can be made by combining many similar datasets from many hospitals around the world. This is in line with open science data, amateur data collection, data processing, and computing [19]. In the end, the results show that the pre-processing methods we looked at are very useful and efficient, even in the simplest setup. It's important to note that the pre-processed dataset without bones has much better accuracy and loss results than the other pre-processed datasets after lung segmentation. So, the extra space for development could be linked to better pre-processing algorithms for: lung segmentation using larger datasets with masks; bone shadow elimination using more complex semantic segmentation techniques applied not only to lungs and body parts outside of them (heart, arms, etc.); as well as for ribs and clavicles inside the lungs; and training itself by making the deep learning network bigger and more complicated, from its current small size of 7 layers to >100 layers like in the most accurate networks like CheXNet, which is used to diagnose other diseases [5]. Work is being done right now to train the more involved models on the bigger pictures, and the results will be shared elsewhere [17]. This is why it's important to think about how to fine-tune datasets and deep learning models, as this can have a big impact on how well the model works [20-22].

### References:

1. National Lung Screening Trial Research Team. Reduced lung-cancer mortality with low-dose computed tomographic screening. *N. Engl. J. Med.*, 365, 395-409 (2023).
2. Owens, J.D., Luebke, D., Govindaraju, N., Harris, M., Krüger, J., Lefohn, A.E., Purcell, T.J. : A survey of general-purpose computation on graphics hardware. In: *Computer graphics forum*, Vol. 26, No. 1, pp. 80-113. Blackwell Publishing Ltd. (2023).
3. Smistad, E., Falch, T.L., Bozorgi, M., Elster, A.C., Lindseth, F. : Medical image segmentation on GPUs - A comprehensive review. *Medical image analysis* 20(1), 18 (2023).
4. LeCun, Y., Bengio, Y., Hinton, G. : Deep Learning. *Nature*, 521(7553), 436-444 (2022).



5. Rajpurkar, P., Irvin, J., Zhu, K., Yang, B., Mehta, H., Duan, T., Ding, D., Bagul, A., Langlotz, C., Shpanskaya, K., Lungren, M.P., Ng, A.Y. : CheXNet: Radiologist-Level Pneumonia Detection on Chest X-Rays with Deep Learning. arXiv preprint arXiv:1711.05225 (2023).
6. Shiraishi, J., Katsuragawa, S., Ikezoe, J., Matsumoto, T., Kobayashi, T., Komatsu, K., Matsui, M., Fujita, H., Kodera, Y., Doi, K. : Development of a Digital Image Database for Chest Radiographs with and without a Lung Nodule: Receiver Operating Characteristic Analysis of Radiologists' Detection of Pulmonary Nodules. American Journal of Roentgenology, 174, 71-74 (2023).
7. Armato, S.G., et al. : The Lung Image Database Consortium (LIDC) and Image Database Resource Initiative (IDRI): a completed reference database of lung nodules on CTscans. Medical Physics, 38(2), 915-931 (2023).
8. Jaeger, S., Candemir, S., Antani, S., Wang, Y.X.J., Lu, P.X., Thoma, G. : Two public chest X-ray datasets for computer-aided screening of pulmonary diseases. Quantitative imaging in medicine and surgery, 4(6), 475 (2022).
9. Jaeger, S., Karargyris, A., Candemir, S., Folio, L., Siegelman, J., Callaghan, F., Zhiyun Xue, Palaniappan, K., Singh, R.K., Antani, S., Thoma, G., Wang, Y.X.J., Lu, P.X., McDonald, C.J. : Automatic tuberculosis screening using chest radiographs. IEEE transactions on medical imaging, 33(2), 233-245 (2022).
10. Wang, X., Peng, Y., Lu, L., Lu, Z., Bagheri, M., Summers, R.M. : Chest X-ray8: Hospital-scale chest X-ray database and benchmarks on weakly-supervised classification and localization of common thorax diseases. arXiv preprint arXiv :1705.02315 (2022).
11. Van Ginneken, B., Stegmann, M.B., Loog, M. : Segmentation of anatomical structures in chest radiographs using supervised methods: a comparative study on a public database. Medical image analysis, 10(1), 19-40 (2022).
12. Hashemi, A., Pilevar, A.H. : Mass Detection in Lung CT Images using Region Growing Segmentation and Decision Making based on Fuzzy Systems. International Journal of Image, Graphics and Signal Processing, 6(1), 1 (2022).

13. Juhász, S., Horváth, Á., Nikhazy, L., Horváth, G. : Segmentation of anatomical structures on chest radiographs. In XII Mediterranean Conference on Medical and Biological Engineering and Computing 2010, pp. 359-362. Springer, Berlin, Heidelberg (2021).
14. Oğul, H., Oğul, B.B., Ağildere, A.M., Bayrak, T., Sümer, E. : Eliminating rib shadows in chest radiographic images providing diagnostic assistance. Computer methods and programs in biomedicine, 127, 174-184 (2021).
15. Ronneberger, O., Fischer, P., Brox, T. : U-net: Convolutional networks for biomedical image segmentation. In International Conference on Medical Image Computing and Computer-Assisted Intervention, pp. 234-241. Springer, Cham (2022).
16. Pazhitnykh I., Petsiuk V. : Lung Segmentation (2D), <https://github.com/imlabuiip/lung-segmentation-2d> (2022).
17. Kochura, Yu., et al. : Data Augmentation for Semantic Segmentation, 10th Int. Conf. on Advanced Computational Intelligence (Xiamen, China) (submitted) (2022).
18. Abadi, M., et al. : Tensor Flow: Large-Scale Machine Learning on Heterogeneous Distributed Systems. arXiv preprint arXiv:1603.04467 (2022).
19. Gordienko, N., Lodygensky, O., Fedak, G., Gordienko, Y. : Synergy of volunteer measurements and volunteer computing for effective data collecting, processing, simulating and analyzing on a worldwide scale. In Proc. IEEE 38th Int. Convention on Information and Communication Technology, Electronics and Microelectronics (MIPRO), pp. 193-198 (2021).
20. Gordienko, N., Stirenko, S., Kochura, Yu., Rojbi, A., Alienin, O., Novotarskiy, M., Gordienko Yu. : Deep Learning for Fatigue Estimation on the Basis of Multimodal Human-Machine Interactions. In Proc. XXIX IUPAP Conference in Computational Physics (CCP2017) (2021).



21. Kochura, Yu., Stirenko, S., Alienin, O., Novotarskiy, M., Gordienko, Yu. : Performance Analysis of Open Source Machine Learning Frameworks for Various Parameters in Single-Threaded and Multi-Threaded Modes. In Conference on Computer Science and Information Technologies, pp. 243-256. Springer, Cham (2020).
22. Rather, N.N., Patel, C.O., Khan, S.A. : Using Deep Learning towards Biomedical Knowledge Discovery. IJMSC-International Journal of Mathematical Sciences and Computing (IJMSC), 3(2), 1 (2019).